SpoIIB Localizes to Active Sites of Septal Biogenesis and Spatially Regulates Septal Thinning during Engulfment in *Bacillus subtilis*

Ana R. Perez, Angelica Abanes-De Mello and Kit Pogliano
J. Bacteriol. **2000, 182(4):1096. DOI: 10.1128/JB.182.4.1096-1108.2000.**

JOURNAL OF BACTERIOLOGY, Feb. 2000, p. 1096–1108 Vol. 182, No. 4
0021-9193/00/$04.00+0

SpoIIB Localizes to Active Sites of Septal Biogenesis and Spatially Regulates Septal Thinning during Engulfment in *Bacillus subtilis*

ANA R. PEREZ, ANGELICA ABANES-DE MELLO, AND KIT POGLIANO*

Department of Biology, University of California, San Diego, La Jolla, California 92093-0349

Received 29 July 1999/Accepted 19 November 1999

A key step in the *Bacillus subtilis* spore formation pathway is the engulfment of the forespore by the mother cell, a phagocytosis-like process normally accompanied by the loss of peptidoglycan within the sporulation septum. We have reinvestigated the role of SpoIIB in engulfment by using the fluorescent membrane stain FM 4-64 and deconvolution microscopy. We have found that *spoIIB* mutant sporangia display a transient engulfment defect in which the forespore pushes through the septum and bulges into the mother cell, similar to the situation in *spoIID*, *spoIIM*, and *spoIIP* mutants. However, unlike the sporangia of those three mutants, *spoIIB* mutant sporangia are able to complete engulfment; indeed, by time-lapse microscopy, sporangia with prominent bulges were found to complete engulfment. Electron micrographs showed that in *spoIIB* mutant sporangia the dissolution of septal peptidoglycan is delayed and spatially unregulated and that the engulfing membranes migrate around the remaining septal peptidoglycan. These results demonstrate that mother cell membranes will move around septal peptidoglycan that has not been completely degraded and suggest that SpoIIB facilitates the rapid and spatially regulated dissolution of septal peptidoglycan. In keeping with this proposal, a SpoIIB-myc fusion protein localized to the sporulation septum during its biogenesis, discriminating between the site of active septal biogenesis and the unused potential division site within the same cell.

Bacillus subtilis is a gram-positive bacterium which, under conditions of nutrient deprivation, undergoes a developmental process known as sporulation (for review, see references 10 and 46). During sporulation, a septum is positioned near the pole instead of the midcell site used for vegetative division, resulting in the production of two daughter cells of different sizes and fates, a smaller forespore and a larger mother cell. Shortly after the onset of differential gene expression in these two cells, the septum between them begins to migrate around the forespore until the leading edges of the membrane meet on the distal side of the forespore and fuse, releasing the forespore into the mother cell cytoplasm (Fig. 1A). After the completion of this phagocytosis-like process (known as engulfment), the forespore is enclosed in the mother cell and bounded by two membranes, its original cytoplasmic membrane and a membrane derived from the engulfing mother cell membrane. It is between these two membranes that the specialized spore cell wall (the cortex) is synthesized, while the multilayered spore coat is assembled around the forespore within the mother cell cytoplasm.

Although engulfment is an essential part of the spore formation pathway of *B. subtilis* and its endospore-forming relatives, the mechanism by which the membranes move around the forespore remains poorly understood. However, it appears that thinning or removal of peptidoglycan between the septal membranes is necessary to allow movement of the mother cell membrane around the forespore (16, 31). Previous electron microscopy studies suggested that septal thinning is initiated from the middle of the septum and proceeds toward the edges (16); the exact mechanism for this process and the means by which it is spatially regulated remain unknown. Five proteins have been implicated in this step of engulfment: SpoIIM, SpoIIP, SpoIID, SpoIIB, and SpoVG (13, 25, 29, 43); three of them, SpoIIM, SpoIIP, and SpoIID, are produced in the mother cell about 1 h after initiation of sporulation (13, 37, 42). Strains lacking any of these three proteins have similar phenotypes, with peptidoglycan dissolution occurring only in the middle of the septum, no migration of the mother cell membrane around the forespore, and a prominent bulging of the forespore into the mother cell. Another phenotype of these strains is the retention of partial septa at the second potential division site in the mother cell; these partial septa also form in the wild type but later regress, a process likely to require removal of peptidoglycan from the partial septa (32). Although no exact function has been ascribed to any of these proteins, the C terminus of SpoIID displays a high degree of homology with LytB, a protein that regulates LytC, a muramidase which is the major *B. subtilis* autolysin (18, 20). Another sporulation protein, which shows homology to cell wall hydrolases, is SpoIIQ, which was first identified as being required for moving the mother cell membrane across the distal pole (24). However, recent work in our lab has shown that the requirement of SpoIIQ for the completion of engulfment is medium dependent and that SpoIIQ may be involved in forespore-specific gene expression (Y.-L. Sun, M. D. Sharp, and K. Pogliano, submitted for publication).

The genes encoding SpoIIB and SpoVG are expressed at the onset of sporulation (29, 38). Previous studies showed that *spoIIB* and *spoVG* single mutants were only mildly impaired for sporulation and appeared to have a wild-type engulfment phenotype while a *spoIIB spoVG* double mutant produced few spores and was blocked at early stages of engulfment, with little or no thinning of septal peptidoglycan (29). SpoIIB shows weak homology to the substrate specificity domain of CwlM, a *Bacillus licheniformis* amidase (19, 29), suggesting that it interacts with the cell wall, while SpoVG shows homology to proteins of unknown function in *Archaeoglobus fulgidus*, *Borrelia*

* Corresponding author. Mailing address: Department of Biology, University of California, San Diego, 9500 Gilman Dr., San Diego, CA 92093-0349. Phone: (858) 822-1314. Fax: (858) 822-1431. E-mail: kpogliano@ucsd.edu.

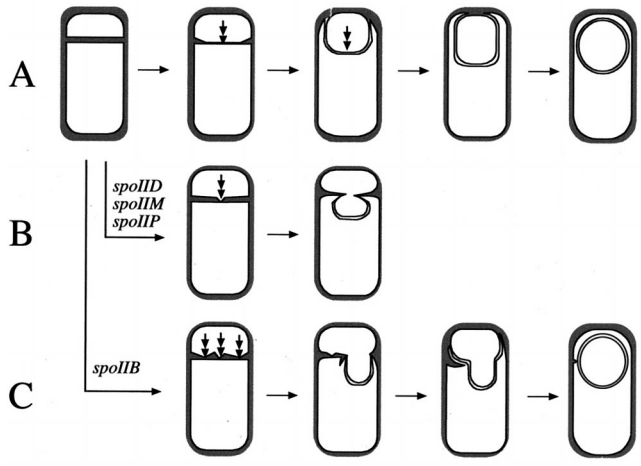

FIG. 1. Model for engulfment in the wild type and in *spoIID*, *spoIIM*, *spoIIP*, and *spoIIB* mutants. (A) Engulfment in the wild type. After polar septation, septal peptidoglycan is degraded, beginning in the middle of the septal disc (arrow) and proceeding toward the edges. The mother cell membranes move up and around the growing forespore (center sporangium), which ultimately becomes fully enclosed within the mother cell (far-right sporangium). (B) Engulfment in *spoIID*, *spoIIM*, and *spoIIP* mutants. As in the wild type, there is initial dissolution of the septal peptidoglycan in the center of the septal disc (left sporangium, arrow); however, degradation is not complete. When the forespore grows, it breaks through this weakened region of the septum, resulting in the bulging of the forespore into the mother cell (right sporangium). (C) Engulfment in *spoIIB* mutants. In *spoIIB* mutants, the septal peptidoglycan is incompletely degraded throughout the septum (left-most sporangium, arrows). When the forespore grows, it breaks this weakened septal peptidoglycan, resulting in broad bulges of the forespore into the mother cell, with peptidoglycan being displaced into the mother cell. Despite this residual peptidoglycan, engulfment is completed.

burgdorferi, *Bacillus megaterium*, and *Clostridium acetobutylicum* (1, 30). It was recently reported that *spoVG* mutant sporangia initiate polar septation more rapidly than wild-type sporangia, suggesting that SpoVG serves directly or indirectly as a repressor of polar septation (30). The reason for the synergy between *spoIIB* and *spoVG* mutations remains unclear.

Here we report the further characterization of the roles of SpoIIB and SpoVG in engulfment. Using a sensitive assay for engulfment, we observed that a *spoIIB* null mutant displays a transient engulfment phenotype not described previously but similar to that of other engulfment mutants which fail to degrade septal peptidoglycan. Ultimately, however, the *spoIIB* mutant is able to complete engulfment, suggesting that the defect affects only the speed of engulfment. In contrast, engulfment proceeds normally in the *spoVG* mutant, suggesting that this gene's product is not directly involved in engulfment. We have also demonstrated that SpoIIB localizes to active sites of septal biogenesis and that its localization is dependent on an as-yet-unidentified structure within the polar septum. Our studies suggest that SpoIIB is necessary for efficient dissolution of septal peptidoglycan.

MATERIALS AND METHODS

Bacterial strains and strain construction. *B. subtilis* strains used in this work are listed in Table 1. Strains were constructed from the prototroph *B. subtilis* PY79 by conventional genetic techniques (8). KP548 was constructed by transforming KP10 with pTn917Ω*strR*, which is able to replace the existing macrolide-lincosamide-streptogramin B resistance marker with a spectinomycin resistance marker following a double-recombination event (44). Construction of strain KP545 is described in the next section. *Escherichia coli* KJ622 (TGI *pcnB24-1*) was constructed by P1 transduction from donor strain MJC97 (*pcnB24-1*::Tn*10*Ω*strR*,*tetS*) to recipient TG1, selecting for the Tn*10* (Str^r) transposon linked to *pcnB* (26), and screening for isolates with low plasmid copy numbers.

TABLE 1. *B. subtilis* strains used in this study[a]

Strain	Genotype	Reference or source
PY79	Prototrophic	51
KP10	*spoVG*::ΩHU265	39
KP52	*spoIIB*Δ::erm *spoVG*::Tn*917*ΩHU265	29
KP69	*spoIIE*::Tn*917*ΩHU7	39
KP174	Δ(*spoIIAA-spoIIAC*)Ω*spc*	Gift from P. Stragier
KP343	*spoIIB*Δ::erm	29
KP444	P_{spac}-*ftsZ*::phleo	4
KP519	*spoIIM*::Tn*917*	39
KP548	*spoVG*::Tn*917*::*spc*	This study
KP545[b]	*spoIIB*-mycΩcm	This study
KP547[b]	P_{spac}-*ftsZ*::phleo *spoIIB*-mycΩcm	This study
KP549[b]	Δ(*spoIIAA-spoIIAC*)Ω*spc spoIIB*-mycΩcm	This study
KP550[b]	*spoVG*::*spec spoIIB*-mycΩcm	This study

[a] All strains are congenic with PY79.
[b] Wild-type *spoIIB* gene replaced with *spoIIB-myc* fusion.

Construction of myc-tagged SpoIIB. Using primers 5′-CTTAGAATTCGGG TTAAACATATCGGG3′ and 5′AATTTCTCGAGTTTTACGACGGCTAAC AG3′, a 612-bp fragment corresponding to the 3′ end of the *spoIIB* coding region was isolated from strain PY79. *Eco*RI (New England Biolabs) and *Ava*I (Boehringer Mannheim) restriction sites (underlined) were introduced to facilitate cloning. *Taq* polymerase (Qiagen) was used under the following conditions to obtain the fragment: an initial denaturation at 94°C for 5 min; 30 cycles of denaturation at 94°C for 1 min, annealing at 47°C for 1 min, and extension at 72°C for 1 min; and a final extension at 72°C for 10 min. The PCR product was purified by using a QIAquick PCR Purification Kit (Qiagen) and digested with *Eco*RI and *Ava*I. The vector plasmid pKL94 (a gift from K. Lemon), encoding a c-myc tag, was linearized with *Eco*RI and *Ava*I. Fragments were purified by using Geneclean II (Bio101); the fragment and vector were then ligated and transformed into strain KJ622 (TGI *pcnB*, described above). PKL94 was isolated by using a Plasmid Midi Kit (Qiagen) and transformed into PY79. A single homologous recombination event integrated the *spoIIB-myc*-containing plasmid at the chromosomal *spoIIB* gene, resulting in strain KP545. Competent KP545 was then transformed with KP444, KP174, and KP548 chromosomal DNA to obtain KP547, KP549, and KP550, respectively.

Resuspension sporulation. Sporulation was induced by the method of Sterlini and Mandelstam (45). The membrane stain FM 4-64 (Molecular Probes) was included in the resuspension medium as described by Pogliano et al. (32). The DNA stain 4′,6-diamidino-2-phenylindole (DAPI) was added to the cells immediately prior to viewing, as described previously (32).

Since KP547 contains FtsZ under the isopropyl-β-D-thiogalactopyranoside (IPTG)-inducible P_{spac} promoter, all samples were grown in the presence of 1 mM IPTG to provide the FtsZ required for cell division. To deplete FtsZ during resuspension sporulation, cells were grown in the presence of 1 mM IPTG until reaching an optical density at 600 nm of 0.2, centrifuged, washed twice in CH medium, and divided in half. One portion was resuspended in CH medium containing 1 mM IPTG, while the other portion was resuspended in CH medium lacking IPTG. The cultures were allowed to grow until the optical density at 600 nm was between 0.5 and 0.6, at which time they were resuspended in sporulation salts with or without (for the depletion) 1 mM IPTG.

Deconvolution and time-lapse microscopy. Deconvolution microscopy and image processing was performed essentially as described by Pogliano et al. (32). However, for time-lapse experiments, cells were grown in the presence of FM4-64 at 1 μg ml^{-1} and images were collected every 20 min. Of the 29 *spoIIB* mutant sporangia that could be monitored throughout the time course, 18 completed engulfment following bulge formation, 1 completed engulfment with no detectable bulging, 4 failed to initiate engulfment, 2 initiated but did not complete engulfment, 3 lysed before the completion of engulfment, and one formed a disporic sporangium. Fields of cells from these time-lapse experiments can be seen on the Pogliano lab website (http://www.biology.ucsd.edu/labs/pogliano).

Immunofluorescence microscopy. Immunofluorescence microscopy was performed as described by Arigoni et al. (2) with the following modifications. A 0.5-ml portion of the sporulating culture was fixed in a solution containing 20 mM sodium phosphate (pH 7.2), 3% (wt/vol) paraformaldehyde, and 0.007% (wt/vol) glutaraldehyde (the last two were obtained from EM Sciences). Samples were fixed for 20 min at room temperature, washed with phosphate-buffered saline three times, and placed on ice for a maximum of 4 h. Sporangia were permeabilized with lysozyme (0.8 mg ml^{-1}) for 4 min and washed with phosphate-buffered saline. Prior to addition of the primary antibody, sporangia were blocked with 2% bovine serum albumin at room temperature for 15 min. Samples were incubated overnight at 4°C with the primary antibodies, an anti-c-myc

mouse antibody (Boehringer Mannheim) at 1.1 μg ml^{-1} and an affinity-purified anti-FtsZ rabbit antibody (a gift from P. Levin, purified by N. Osborne) at 1:500. Slides were washed with phosphate-buffered saline and then incubated with the secondary antibodies, an affinity-purified fluorescein isothiocyanate (FITC)-labeled donkey anti-mouse antibody (at 5 μg ml^{-1}) and an affinity-purified Cy5-labeled donkey anti-rabbit antibody (at 5 μg ml^{-1}) (both from Jackson Immunolabs), at room temperature for 3 h. DAPI (0.2 μg ml^{-1}; Molecular Probes) and FM 4-64 (10 μg ml^{-1}; Molecular Probes) were added with the equilibration buffer. We noted that FM 4-64 bleached rapidly in fixed cells exposed to UV irradiation. Therefore, before collecting images of fluorescein fluorescence, we bleached the FM 4-64, using a DAPI filter set to ensure that there was no FM 4-64 fluorescence remaining (which otherwise might be visualized together with fluorescein). To ensure that FM 4-64 did not affect protein localization, control experiments were performed without the stain; identical results were obtained. A wild-type strain, PY79, without the c-myc fusion was used as a negative control; it showed faint, punctate staining that did not localize to the septa (data not shown).

Electron microscopy. Sporulating cultures of PY79 and KP343 were prepared for electron microscopy by four methods, three of which are slight modifications of a protocol frequently used for preparation of *B. subtilis* (32). The fourth method was devised to allow better visualization of the engulfing membranes, which were often obscured by the darkly stained cell wall in the first three methods. Method I exactly followed a previously described protocol (32) which employed a fixation with 4% (wt/vol) glutaraldehyde in 0.1 M sodium phosphate (pH 7.0) followed by a secondary fixation with 1% (wt/vol) osmium tetroxide in 0.1 M sodium phosphate (pH 7.0) and then a wash in 0.5 M ammonium chloride (see Fig. 4A, C, I, and M to O). Method II introduced the 0.5 M ammonium chloride wash before (rather than after) the osmium tetroxide fixation (see Fig. 4B, E to H, L, and R), whereas method III lacked the ammonium chloride wash (see Fig. 4D). Following agarose enrobing, Spurr's resin embedding, and ultrathin sectioning, the samples were poststained with 1% (wt/vol) uranyl acetate in 30% (vol/vol) ethanol and Reynold's lead as described previously (32). Method IV was a slight modification of a protocol used to enhance membrane staining in other organisms (14). Sporangia were fixed for 8 to 14 h at 4°C in 0.1 M sodium cacodylate buffer (pH 7.4) containing 4% (wt/vol) glutaraldehyde and 2 mM calcium chloride. Cells were postfixed for between 8 and 14 h at 4°C in 0.1 M sodium cacodylate buffer (pH 7.4) containing 1% (wt/vol) osmium tetroxide and 3.0% (wt/vol) potassium ferricyanide. Samples were enrobed in agarose, diced, and stained with 1% (wt/vol) uranyl acetate in 30% (vol/vol) ethanol for 8 to 14 h at 25°C. They were embedded in Spurr's resin, which was allowed to polymerize at 65°C for at least 48 h. Ultrathin sections were applied to a grid and poststained with 0.25% (wt/vol) potassium permanganate and Reynold's lead as described elsewhere (14). This protocol was utilized because we were not interested in defining cytoplasmic contents (such as ribosomes) that stain darkly with uranyl acetate and Reynold's lead, obscuring the membranes. We found that this last method readily allowed visualization of the engulfing membranes (see Fig. 4J, K, P, and Q).

Western blot analysis. Western blotting was performed as described by Pogliano et al. (34), with the exception that trichloroacetic acid was not added to the cell suspension. After addition of the 2× sodium dodecyl sulfate loading buffer to the lysozyme-treated cells, samples were heated for 10 min at 80°C and then either used immediately or placed at −70°C for storage. A 30-μl aliquot of sample was electrophoresed in a 12.5% polyacrylamide gel. Following electrophoresis, the gel was equilibrated in Towbin's buffer (25 mM Tris, 192 mM glycine, 20% [vol/vol] methanol, pH 8.3) and transferred onto an Immobilon P transfer membrane (Millipore) by using a Trans-Blot SD semidry transfer cell (Bio-Rad) at 15 V for 45 min. After being blocked, the membrane was incubated overnight at 4°C with a 40-μg ml^{-1} solution of mouse anti-c-myc antibodies (Boehringer Mannheim) or a 1:500 dilution of affinity-purified rabbit anti-FtsZ antibodies. Horseradish peroxidase-labeled anti-mouse or anti-rabbit secondary antibodies (Amersham) were used at a 1:1,500 dilution and incubated with the membrane for 1 h at room temperature. Enhanced chemiluminescence (ECL; Amersham) was used for Western blot analysis.

Measurements of sporangia during engulfment. Wild-type (PY79) sporangia were analyzed from three progressions (reference 32 and this work [time-lapse microscopy of wild-type controls] [see the Pogliano lab website {http://www.biology.ucsd.edu/labs/pogliano} for fields of cells used in these experiments]) by using NIH Image 1.61.1 software. TIFF-formatted images (see sections on microscopy and image analysis in reference 32) were imported into NIH Image; the image shading was inverted (to black membranes on a white background), and the images were processed to display membrane edges. This process represents solid membranes as bilayers, and therefore careful measurements were taken in between the bilayers perpendicular to, and in the middle of the polar septum as follows: to determine sporangial length, measurements were taken across the sporangium, from one pole to the opposite pole; to determine forespore growth, measurements were taken from the middle of the polar septum to the proximate pole; and to represent mother cell size, measurements were taken from the middle of the polar septum to the distal pole. Only sporangia which were flat, as indicated by the clear visualization of both ends of the sporangium without blurring, were scored. Twenty-three sporangia from the first and last time points were measured. While the forespore grew by an average ± standard deviation of 21.9% ± 11.9%, the combined length of both cells decreased slightly, by an average of 1.5% ± 3.1%. One sporangium was excluded from the data analysis because it had an unusual phenotype at the 1-h time point.

RESULTS

The *spoIIB* mutant shows a transient engulfment phenotype. The SpoIIB protein was predicted to be involved in the early stages of engulfment (29) based on the phenotype of a *spoIIB spoVG* double mutant, although neither mutation alone resulted in an obvious engulfment defect. To determine whether either *spoIIB* or *spoVG* mutations alone caused a subtle, not previously identified engulfment defect, we used the vital membrane stain FM 4-64 to investigate engulfment at early times in the spore formation process. When used with deconvolution microscopy, FM 4-64 clearly reveals the sporulation septum before, during, and after engulfment, without notably affecting either growth or sporulation (32). Cultures were grown in the presence of FM 4-64 and induced to sporulate by resuspension, and samples were taken 2, 3, and 4 h after the onset of sporulation ($t_{2.0}$, $t_{3.0}$, and $t_{4.0}$, respectively). The bacteria were stained with DAPI and prepared for deconvolution microscopy as described previously (32) (see Materials and Methods). In wild-type sporangia, the sporulation septum appeared flat shortly after its biogenesis (32) (data not shown). At the onset of engulfment, the sporulation septum began to curve around the smaller forespore (Fig. 2A, arrow 1) moving up the sides of the forespore (Fig. 2A, arrow 2) until the forespore was completely surrounded by the engulfing membranes (Fig. 2A, arrow 3). During, and shortly after engulfment, the forespore chromosome stained brightly with DAPI and appeared to be more fully condensed than the mother cell chromosome (40) (Fig. 2B, arrow). By $t_{2.0}$, approximately 50% of wild-type sporangia had completed engulfment (Table 2), while 1 h later (at $t_{3.0}$), 72% had completed engulfment (Fig. 2C and D; Table 2).

Engulfment was completed much more slowly in *spoIIB* mutant sporangia than in those of the wild type; by $t_{2.0}$, only 4% of *spoIIB* mutant sporangia had completed engulfment (Fig. 1E and F; Table 2). Also, 25% of *spoIIB* mutant sporangia showed bulging of the forespore into the mother cell, as evidenced by the displacement of the sporulation septum into the mother cell, resulting in the formation of sags or bubbles of septal membranes (Fig. 2E, arrow). In wild-type sporangia, bulging of the forespore into the mother cell is rarely observed by FM 4-64 staining (zero bulges in >1,500 sporangia at $t_{1.5}$, 1.8% at $t_{2.0}$); when bulges are seen, they are less prominent than those in *spoIIB* mutant sporangia. However, a similar bulging phenotype is observed in other engulfment mutants, such as *spoIIM* (Fig. 2S, arrow) (43), *spoIID* (25), and *spoIIP* (13). We noted three differences between bulges in these mutants and those in *spoIIB* mutants. First, the bulges are somewhat more centrally located in *spoIIM* (Fig. 2S), *spoIID*, and *spoIIP* mutants than in *spoIIB* mutants (Fig. 2E). Second, the forespore bulges in *spoIIM* (Fig. 2S) (43), *spoIID* (25, 32), and *spoIIP* (13) mutants contain a striking constriction at the septum that is less prominent in *spoIIB* bulges (Fig. 2E). Finally, in many *spoIIB* mutant sporangia with bulging forespores, the engulfing membranes appeared to have partially migrated around the forespore (Fig. 2E, arrow). Migration of the septal membranes around the forespore does not occur in *spoIIM*, *spoIID*, or *spoIIP* mutant sporangia (13, 25, 43) (Fig. 2S), which instead begin lysing approximately 3 to 4 h after the onset of sporulation (31, 43) (confirmed by our observations). We also noted that the chromosomes in the bulging forespores of *spoIIB*, *spoIIM*, *spoIID*, and *spoIIP* mutants often appeared unusual in that they were sometimes partitioned between the

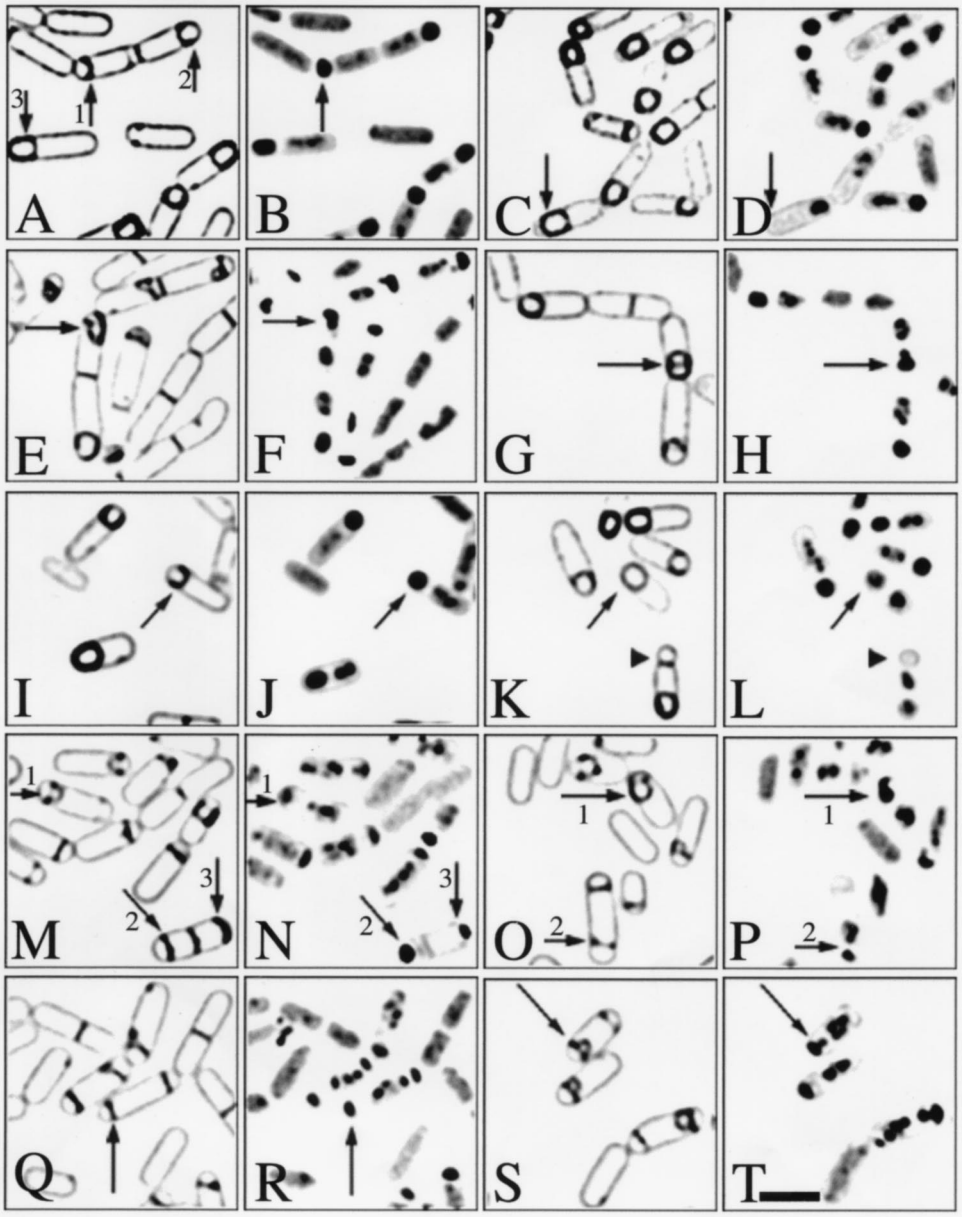

FIG. 2. Analysis of *B. subtilis* engulfment mutants, using FM 4-64 to visualize membranes. Sporangia were treated with the vital membrane stain FM 4-64 (first and third columns) and the DNA stain DAPI (second and fourth columns) and prepared for deconvolution microscopy as described in Material and Methods. (A and B) PY79 (wild type), 2 h after onset of sporulation ($t_{2.0}$). The asymmetrically positioned sporulation septum (panel A, arrow 1) initially stains approximately twofold more brightly with FM 4-64 than the cytoplasmic membrane because it contains two parallel membranes. The forespore chromosome stains more brightly with DAPI and appears more highly condensed (panel B, arrow) than the mother cell chromosome. During engulfment, the septal membrane wraps around the smaller forespore (panel A, arrow 2) until it is completely enclosed within the cytoplasm of the larger mother cell (panel A, arrow 3). (C and D) PY79 (wild type) at $t_{3.0}$. After the completion of engulfment (C) (arrow), DAPI is excluded from the forespore (D) (arrow), for reasons that are as yet unclear (32). (E and F) KP343 (*spoIIB*) at $t_{2.0}$. The arrows point to a *spoIIB* mutant in which the septum bulges into the mother cell (E), with the forespore chromosome partitioned between the forespore and the forespore bulge (F). (G and H) KP343 (*spoIIB*) at $t_{3.0}$. The arrows indicate a *spoIIB* mutant sporangium that appears to have completed engulfment and which retains a partitioned forespore chromosome. (I and J) KP10 (*spoVG*) at $t_{2.0}$. Engulfment proceeds normally in *spoVG* mutant sporangia. (K and L) KP10 (*spoVG*) at $t_{3.0}$. The arrows indicate a *spoVG* mutant sporangium that has completed engulfment; the arrowheads indicate an aberrant division that is producing an anucleate cell at the forespore distal pole of the mother cell. (M and N) KP52 (*spoIIB spoVG*) at $t_{2.0}$. Arrows 1 indicate a *spoIIB spoVG* double-mutant sporangium in which the forespore bulges into the mother cell. Arrows 2 and 3 point to the two forespores in a sporangium, similar to a disporic sporangium but with an extra septum in the mother cell. The forespore indicated by arrows 3 appears to have collapsed. (O and P) KP52 (*spoIIB spoVG*) at $t_{3.0}$. Arrows 1 indicate a sporangium with a large side bulge. Arrows 2 indicate an unusual sporangium in which an anucleate minicell has formed at one pole (upper portion of sporangium) while a partial septum has formed at the other pole (arrow 2). (Q and R) KP519 (*spoIIM*) at $t_{2.0}$. The arrows point to a partially disporic sporangium which contains two forespores; one (arrow) contains a fully translocated chromosome, while in the second, DNA translocation is incomplete. Similar partially disporic sporangia are also seen in *spoIID* and *spoIIP* mutants (32). (S and T) KP519 (*spoIIM*) at $t_{3.0}$. The arrows indicate the medial bulge seen in *spoIIM* as well as other engulfment mutants, such as *spoIID* and *spoIIP*; this sporangium also has a partial septum at the forespore distal pole and is therefore partially disporic. The bar in panel T represents 2 μM.

TABLE 2. Engulfment phenotypes of various *B. subtilis* strains as assessed by FM 4-64 membrane staining and fluorescence microscopy at the indicated times of the sporulation process

Engulfment phenotype	% of sporangia exhibiting phenotype at indicated time for genotype[a]:											
	wt		*spoIIB*		*spoVG*		*spoIIB spoVG*		*spoIIM*	
	t_2	t_3	t_2	t_3	t_2	t_3	t_2	t_3	t_2	t_3
Straight and curved[b]	40.2 (111)	24.9 (66)	49 (438)	30.3 (108)	51.5 (83)	26.0 (51)	50.2 (312)	35.8 (141)	56.4 (269)	36.3 (174)
Engulfed[c]	51.8 (143)	71.7 (190)	3.9 (35)	26.1 (93)	36.6 (59)	62.1 (113)	1.1 (7)	3.7 (11)	0 (0)	0 (0)
Bulge[d]	1.1 (3)	0.4 (1)	20.4 (182)	26.7 (95)	0.0 (0)	0.0 (0)	15.0 (93)	18.5 (73)	7.3 (35)	26.5 (127)
Dispore[e] with bulge[f]	0.7 (2)	0.0 (0)	4.7 (42)	2.8 (10)	0.0 (0)	0.5 (1)	4.0 (25)	5.3 (21)	7.5 (36)	15.4 (74)
Disporic[e]	4.7 (13)	0.8 (2)	15.8 (141)	6.2 (23)	6.8 (11)	5.0 (9)	22.7 (141)	19.8 (78)	27.0 (129)	20.5 (98)
Abnormal division[g]	0.7 (2)	0.8 (2)	3.0 (27)	2.2 (8)	3.7 (6)	3.3 (6)	4.3 (27)	6.6 (26)	0 (0)	0 (0)
Collapse[h]	0.4 (1)	1.1 (3)	2.3 (21)	5.1 (18)	1.2 (2)	1.6 (3)	2.7 (17)	11.2 (44)	1 (5)	0.6 (3)
Other	0.4 (1)	0.4 (1)	0.3 (3)	0.3 (1)	0.0 (0)	0.0 (0)	0.0 (0)	0.0 (0)	0.6 (3)	0.6 (3)
Total no. of cells scored	566	445	1,670	627	391	381	1,072	643	943	756

[a] The number of sporangia in each phenotypic class was divided by the total number of sporangia (those containing forespores at any stage of engulfment, visualized by FM 4-64 staining). At $t_{2.0}$ and $t_{3.0}$, averages of 50.4 and 57.8%, respectively, of the bacteria in the culture were sporangia. The total numbers of sporangia scored for each class are given in parenthesis. wt, wild type.
[b] Flat and curved polar septa, including those in which the septa had migrated slightly toward the poles.
[c] Those in which the engulfing membranes appear to fully, or almost fully, encircle the forespore.
[d] Those showing a bulging of the forespore into the mother cell.
[e] Disporic sporangia include those with two complete septa and two fully translocated forespore chromosomes (which were not observed in the wild type) and those with one complete septum (with a fully translocated forespore chromosome) and one partial septum with an incompletely translocated forespore chromosome (for an example, see Fig. 1Q and R, arrow).
[f] Disporic sporangia in which one polar septum bulges into the mother cell (for an example, see Fig. 1S and T, arrow).
[g] Sporangia containing an extra septum at midcell, resulting in anucleate mother cells (for an example, see Fig. 2M, arrows 2 and 3).
[h] Forespores in which the membranes and DNA appear compressed against the pole of the sporangium (for an example, see Fig. 2M and N, arrow 3).

FIG. 3. Time-lapse deconvolution microscopy of engulfment in *spoIIB* mutant sporangia. A culture of KP343 (*spoIIB*) was grown in the presence of FM 4-64, and sporulation was induced by resuspension. At 1.5 h after the initiation of sporulation, the culture was affixed to a coverslip (see Materials and Methods). Images were collected every 20 min over a period of 1 h, as indicated by the time line above the sporangia. The panels of this figure display a progression of three different sporangia, from polar septation (A and B) or bulge formation (C) through recovery of the bulge and, finally, completion of engulfment. The fields from which these examples were taken are presented in the Pogliano lab website (http://www.biology.ucsd.edu/labs/pogliano). The bar in panel C represents 2 μM.

forespore bulge and the forespore (Fig. 2F and T, arrows). By $t_{3.0}$ (Fig. 2G), approximately 26% of *spoIIB* mutant sporangia had completed engulfment (Fig. 2G and H). Some of the engulfed sporangia contained a slight medial constriction (Fig. 2G, arrow) and retained the partitioned forespore chromosome seen in the sporangia containing bulges at $t_{2.0}$ (Fig. 2H, arrow), suggesting that these sporangia had completed engulfment after the formation of a forespore bulge.

Time-lapse microscopy of engulfment in a *spoIIB* mutant. The results described above suggested that engulfment in *spoIIB* mutant sporangia is preceded by the bulging of the forespore into the mother cell. To demonstrate that sporangia with bulges are capable of completing engulfment, we performed time-lapse deconvolution microscopy of FM 4-64-stained *spoIIB* mutant sporangia, using a method previously described (32) (Fig. 3). Sporangia were applied to a coverslip 90 min after the onset of sporulation, and images were collected every 20 min for 1 h. At the first time point, many sporangia had completed polar septation (Fig. 3A and B) and some showed bulging of the forespore into the mother cell (Fig. 3C). At the second time point, the two sporangia that initially had flat polar septa showed a bulging of the forespore into the mother cell (Fig. 3A and B, 20-min time point), while engulfment was under way in the sporangium that had started with a bulge (Fig. 3C, 40-min time point) (see the Pogliano lab website [http://www.biology.ucsd.edu/lab/pogliano] for fields of sporangia from these time-lapse experiments). By the end of the time course, 19 of 29 sporangia had completed engulfment; in 18 of these 19, a forespore bulge was evident at one or more time points. Thus, although prominent bulging of the forespore into the mother cell is not normally part of the engulfment pathway in *B. subtilis*, this event does not inhibit the successful completion of engulfment in *spoIIB* mutant sporangia.

Transmission electron microscopy analysis. To determine more precisely the septal structure of *spoIIB* mutants during the process of engulfment, we performed transmission electron microscopy on cultures harvested at $t_{2.0}$, a time at which bulges are prevalent. After polar septation, a layer of peptidoglycan lies between the septal membranes (16) (Fig. 4A). In the wild type, the septal peptidoglycan is thinned, apparently beginning in the middle of the septum (Fig. 4B, arrowhead) and moving toward the edges of the septum (16, 31) (Fig. 4C, arrowhead). Once the peptidoglycan is completely removed (Fig. 4D), the mother cell membranes move up and around the forespore (Fig. 4E and F) until the forespore is completely enclosed within the mother cell cytoplasm (Fig. 4G). In *spoIIB* mutant sporangia, the thickness of the peptidoglycan between the mother cell and forespore membranes often appeared uneven across the septum (Fig. 4I, J, L, and M, arrowheads), although occasionally septal thinning appeared more similar to that seen in the wild type (Fig. 4K). These observations suggested that in *spoIIB* mutants, thinning of the septal peptidoglycan occurred randomly throughout the septum. Bulges of the forespore into the mother cell occurred both at the middle (Fig. 4N) and the edges (Fig. 4O and P) of the septum. Often the septal peptidoglycan in these sporangia was displaced from the original plane of the septum into the mother cell (Fig. 4N to P, arrowheads), appearing to have been pushed aside as the forespore bulged into the mother cell. Occasionally, fragments of septal peptidoglycan were observed on the forespore bulge (Fig. 4N, double arrowhead). This was in contrast to the situation in the wild type, in which neither large forespore bulges nor folds of cell wall material were observed. In *spoIIB* mutant sporangia, engulfment occurred around residual septal peptidoglycan, which often extended almost 200 nm into the middle of the cell (Fig. 4P and Q). A large amount of septal peptidoglycan remained after engulfment was complete (Fig. 4R), perhaps explaining the medial constriction of the engulfed forespore shown in Fig. 2G and H (arrow). Thus, septal thinning appeared to be spatially unregulated in *spoIIB* mutant sporangia and was not complete prior to the onset or completion of engulfment.

The *spoVG* and *spoIIB spoVG* mutant phenotypes. Since the *spoVG* mutation enhances the sporulation deficiency of *spoIIB* mutations (29), we next examined the *spoVG* single-mutant and the *spoIIB spoVG* double-mutant phenotypes by FM 4-64 membrane staining. The *spoVG* single mutant has been shown to display an early onset of polar septation (30), mild impairment of cortex synthesis (38), and a slight decrease in sporulation efficiency (29, 38). We found that at early times in the spore formation process, the ability of the *spoVG* single mutant to initiate and complete engulfment appeared similar to that of the wild type (Fig. 2I to L). We did not observe any sporangia with the bulging phenotype characteristic of an early engulfment defect, and engulfment was completed at about the same rate as in the wild type (Table 2). We also observed that about 10% of *spoVG* mutant sporangia display aberrant divisions, such as the minicell forming in the sporangium in Fig. 2K, as well as other division phenotypes, which will be described below.

As previously reported (29), the *spoIIB spoVG* double mutant displays a strong impairment of engulfment (Fig. 2M to P). However, in addition to the flat polar septa previously described, we observed bulges of the forespore into the mother cell (Fig. 2M, arrow 1), some of which appeared to have initiated but not completed engulfment (Fig. 2O, arrow 1). Indeed, 2 h after the onset of sporulation, 50.2% of sporangia had a flat polar septum while sporangia that had the bulging phenotype accounted for 19.0% of the population. One hour later (at t_3), the population of sporangia was similar to that observed at t_2 (Table 2) and the bulging sporangia appeared to be lysing. This may explain why the bulging phenotype was not observed previously, since samples for electron microscopy were taken 4 h after induction of sporulation (29).

We also noted that 26% of *spoIIB spoVG* double-mutant sporangia (and, at a lower frequency, *spoVG* single-mutant sporangia) contained additional septa, either at polar or medial sites. Additional polar division events have been described in sporangia lacking the activity of the mother cell transcription factor σ^E (16, 31, 40). In such sporangia, division occurs at both potential sites of polar septation, resulting in the production of disporic sporangia with two forespore compartments, each with a chromosome, and a centrally located and anucleate mother cell (23, 32, 40). A second example is provided by the engulfment mutants *spoIID*, *spoIIM*, and *spoIIP*, which produce partially disporic sporangia (32). Such sporangia contain one forespore with a chromosome, while at the second potential site of polar septation a septum (often incomplete) forms, but the chromosome is incompletely segregated into this second forespore (Fig. 2Q and R, arrow).

The *spoIIB spoVG* double-mutant division phenotype was distinct from these two previous examples, since the extra septa were positioned at midcell as well as at polar division sites. Thus, anucleate mother cells, forespores, and minicells were produced. For example, the sporangium indicated by arrows 2 and 3 in Fig. 2M and N appears to have two forespores and two centrally located, anucleate mother cells between the forespores. Such a sporangium could be produced if, following formation of one polar septum, division occurred again at midcell and at the remaining polar division site, with the chromosome ultimately being translocated into the second forespore. The disporic sporangia produced by the *spoIIB spoVG* double mutant fell into several classes differing in the positioning and number of chromosomes. First, as in the classic dispores produced by σ^E-defective sporangia, some of the *spoIIB spoVG* dispores contained two forespores, each with a single chromosome and an anucleate mother cell (data not shown). Others appeared similar to the partial dispores of engulfment mutants, in which the second forespore septum was often incomplete and contained part of a chromosome. Finally, some dispores had an anucleate forespore (these perhaps should more precisely be called minicells) and one or two chromosomes with various degrees of segregation into the second forespore (Fig. 2O and P, arrow 2).

Another significant phenotype (exhibited by 11% of the sporangia at $t_{3.0}$) in the double mutant was strong membrane staining near one pole of the sporangium and a highly condensed, and often crescent-shaped chromosome at the same site (Fig. 2M and N, arrow 3). We suggest that these represent collapsed forespores and may be identical to the pygmy sporangia previously described for the *spoVM ftsH* double mutant (7).

Localization of SpoIIB-myc to the sporulation septum. Because it appeared that SpoIIB is necessary for the efficient degradation of septal peptidoglycan, we next investigated its subcellular distribution. To do so, we constructed a fusion gene encoding an epitope-tagged SpoIIB-myc protein and used antibodies directed against the c-myc epitope to localize the fusion protein by indirect immunofluorescence microscopy. The *spoIIB*-myc fusion gene replaced the wild-type *spoIIB* gene and was able to support wild-type levels of spore formation (data not shown), with no aberrant sporangia being produced at early or late times of sporulation (data not shown).

The SpoIIB-myc fusion protein was visualized by using mouse monoclonal antibodies directed against the c-myc

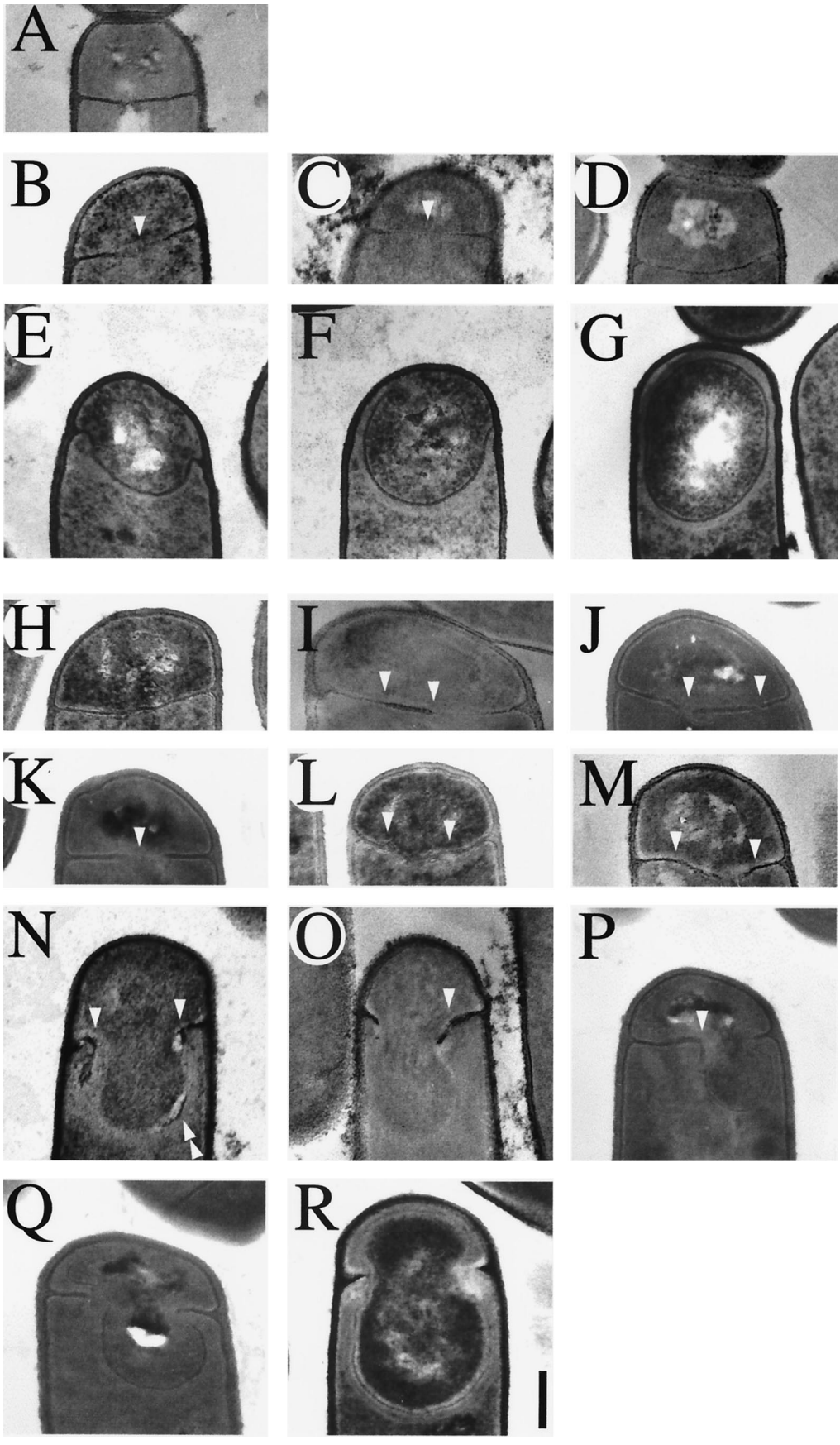

epitope and FITC-labeled secondary antibodies (green), while FM 4-64 (red) and DAPI (blue) were used to visualize membranes and DNA, respectively. Although membrane structure is not as well-defined in immunofluorescence experiments as it is in living cells, the polar septum could be readily visualized prior to the onset of engulfment (Fig. 5C, arrow) and after the completion of engulfment (Fig. 5G, arrow 3). The DAPI-stained chromosomes shown in Fig. 5 appear more punctate than in many previous publications, a difference we attribute to our use of an optical sectioning deconvolution microscope as well as to differences in handling of the micrographs in image processing programs such as Adobe Photoshop (as illustrated in the Pogliano lab website [http://www.biology.ucsd.edu/labs/pogliano]). Ninety minutes after the onset of sporulation, SpoIIB-myc localized to the sporulation septum, appearing evenly distributed throughout the septum prior to the onset of engulfment (Fig. 5A to D, arrow). For example, in the sporangium indicated by the arrow in Fig. 5B, SpoIIB-myc (green) localized between the forespore and mother cell chromosomes (Fig. 5A); when SpoIIB-myc staining was overlaid on the FM 4-64 membrane staining in Fig. 5D, SpoIIB-myc was seen to localize to the sporulation septum (yellow). The random punctate immunostaining within the sporangia was also observed in a strain lacking the SpoIIB-myc fusion, although septal staining was absent. We therefore attribute the punctate signal to nonspecific binding of either the primary antibodies or the fluorescently labeled secondary antibodies. The majority of sporangia with flat polar septa showed SpoIIB-myc localization to the septum, while those with curved septa and those in which engulfment was complete failed to show SpoIIB-myc localization (Fig. 5E to H, arrows 2 and 3; scored in Fig. 6). These results suggest that SpoIIB, which is synthesized prior to polar septation, rapidly localizes to newly formed septa and disappears as engulfment commences.

Because genetic evidence suggested that SpoVG and SpoIIB interact (29), we investigated the localization of SpoIIB-myc in *spoVG* mutant sporangia. We found that SpoIIB-myc localized and delocalized similarly to the wild type, with the exception that SpoIIB-myc localized to both poles of *spoVG* dispores (data not shown).

SpoIIB localization is inhibited in FtsZ-depleted cells. We next investigated whether localization of SpoIIB depends on the cell division protein FtsZ. FtsZ plays a central role in bacterial cell division, directing other cell division proteins to the division site (5, 6, 9, 11, 27, 28, 47, 48) and forming a ring that constricts as the septum is synthesized (5). To test whether localization of SpoIIB depends on FtsZ, we examined SpoIIB-myc localization in a strain in which the *ftsZ* gene is under the control of the inducible *spac* promoter (4). In such a strain, FtsZ can be depleted by growth in the absence of IPTG, resulting in the inhibition of cell division and the production of filamentous cells. When FtsZ was depleted during sporulation, SpoIIB-myc failed to localize (Fig. 5U to X), although, as will be discussed later, the protein was present in such sporangia. In contrast, normal SpoIIB-myc localization was observed following induction of FtsZ by IPTG (data not shown). Thus, FtsZ assembly is required for SpoIIB localization.

SpoIIB colocalizes with FtsZ at sites of septal biogenesis. The rapid, FtsZ-dependent localization of SpoIIB-myc to the sporulation septum raised the possibility that SpoIIB-myc assembled into the sporulation septum during its biogenesis. To test this possibility, we colocalized SpoIIB-myc and the cell division protein FtsZ by immunofluorescence microscopy. In the early sporangium, FtsZ localizes in rings to the two potential sites of polar septation (21) but becomes active at only one site, where it constricts during septal biogenesis (5). If SpoIIB localized only to complete septa, SpoIIB-myc and FtsZ should not colocalize; however, if SpoIIB localized to partial septa, then colocalization of SpoIIB-myc and FtsZ would be observed, although SpoIIB-myc would show unipolar localization while FtsZ would show bipolar localization.

Sporulation was induced by resuspension, and samples were prepared for immunofluorescence microscopy 1.5 and 2.5 h after the onset of sporulation. SpoIIB-myc was detected by using mouse monoclonal antibodies directed against the c-myc epitope and FITC-labeled secondary antibodies (green fluorescence, Fig. 5J, L, N, P, R, and T). FtsZ was detected by using affinity-purified rabbit antibodies directed against FtsZ and Cy5-labeled secondary antibodies (far-red fluorescence—false-colored red in Fig. 5K, L, O, P, S, and T). To correlate SpoIIB-myc and FtsZ localization with septal morphology and forespore chromosome segregation, we simultaneously visualized membranes with FM 4-64 (data not shown) and DNA with DAPI (blue fluorescence in Fig. 5I to T). We observed colocalization of SpoIIB-myc and FtsZ in 39% of the sporangia that had incompletely translocated chromosomes and flat polar septa (Fig. 5I to L; scored in Fig. 6); we infer that in these sporangia the sporulation septum was incomplete. In most of these sporangia, FtsZ showed bipolar staining (Fig. 5K, arrow and arrowhead) while SpoIIB-myc showed unipolar staining at the sporulation septum (Fig. 5J, arrow). Most of the remaining sporangia with flat polar septa showed localization of SpoIIB-myc but not FtsZ to the septum (data not shown; scored in Fig. 6); we infer that biogenesis of the sporulation septum was complete in these sporangia. None of the sporangia with curved septa showed localization of FtsZ to the septum, while 42% showed localization of SpoIIB-myc to the septum and the remaining 58% lacked both FtsZ and SpoIIB staining (Fig. 6). Thus, SpoIIB colocalizes with FtsZ at sites of polar septation but does not localize to the inactive FtsZ complex within the same cell. This suggests that SpoIIB localizes to the site of

FIG. 4. Examination of *spoIIB* sporangia by transmission electron microscopy. Strains PY79 (wild type) and KP343 (*spoIIB*) were induced to sporulate by resuspension, and samples taken either 2 h (A to H, J to M, and O to Q) or 3 h (I, N, and R) after the onset of sporulation. Samples were prepared for electron microscopy by protocols described in Materials and Methods. (A to G) Various stages of engulfment in the wild type. The sporulation septum initially contained darkly staining cell wall material (A), which became thinner (as indicated by arrowheads), apparently starting in the middle of the septal disc and proceeding toward the edges (B and C). When septal thinning was complete (D), the forespore and mother cell septal membranes were very close to one another. Engulfment commenced with a slight bowing of the septum (E), and the mother cell membrane migrated around the forespore (F), which ultimately was fully enclosed within the mother cell cytoplasm (G). (H to R) Various stages of engulfment in *spoIIB* mutants. In *spoIIB* mutant sporangia, the septum also initially contained a layer of darkly staining cell wall material (H), and septal thinning (indicated by arrowheads) occasionally started in the middle of the septum (K). However, more frequently, the septum was thinned in several different locations (I and J), and occasionally large regions of the septum appeared incompletely thinned (L and M) (area between arrowheads). In sporangia that contained bulges of the forespore into the mother cell, portions of the darkly staining septal cell wall material were often displaced from the original plane of the septum into the mother cell (N, O, and P) (arrowheads), and sometimes fragments of cell wall material were observed (N) (double arrowhead). This was not observed in wild-type sporangia, in which the septal peptidoglycan was completely thinned before the onset of engulfment. The engulfing membranes moved around residual cell wall material that extended well into middle of the cell (Q), and after engulfment was complete (R), a substantial amount of septal peptidoglycan remained, which we failed to observe in our wild-type strain. The bar in panel R represents 200 nm.

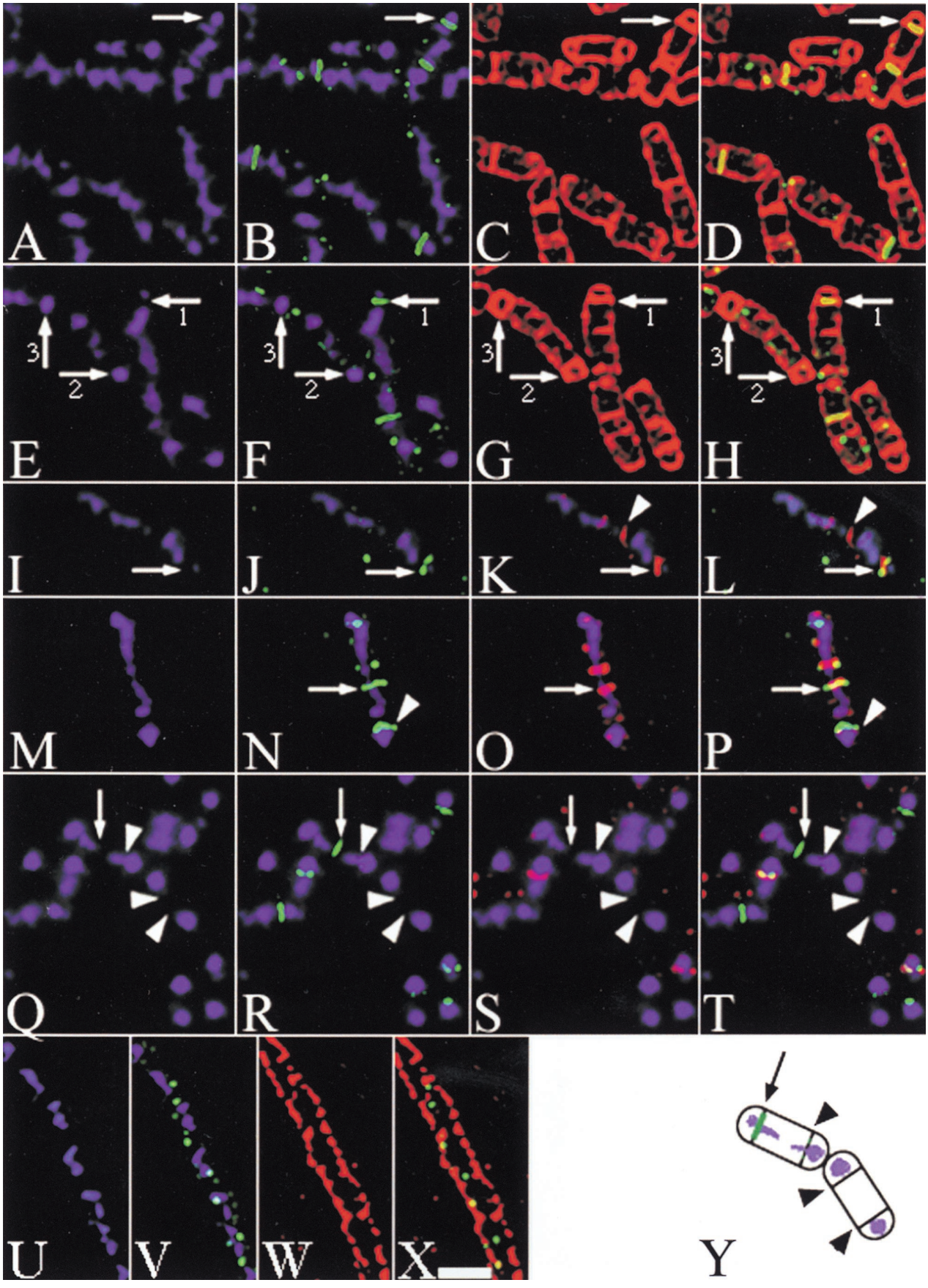

polar septation either shortly before or after the onset of septal biogenesis.

Neither σ^F- nor σ^E-directed gene expression is required for localization or delocalization of SpoIIB. Shortly after polar septation, σ^F becomes active in the forespore, directing the activation of σ^E in the mother cell, thereby allowing the production of proteins essential for hydrolysis of septal peptidoglycan and for engulfment. We were interested in knowing whether either the assembly or disassembly of SpoIIB at the septum depends on proteins under the control of these transcription factors. We therefore examined localization of SpoIIB-myc in two strains, the first containing an insertion mutation in *spoIIGB* (encoding σ^E) and the second containing a deletion of *spoIIAA-AC* (encoding σ^F). Both strains lack σ^E activity and thus divide sequentially at the two polar sites of FtsZ assembly (15, 23, 32), with rapid initiation of division at the second FtsZ ring following completion of the first septum (32). They also sequentially translocate a chromosome into each forespore following division (15, 23, 32). Identical results were obtained for the two strains; here we present only those of the mutant lacking the σ^F protein. After synthesis of the first sporulation septum, SpoIIB-myc (green) localized to this septum (Fig. 5N, arrowhead), as in the wild type. However, SpoIIB-myc also colocalized with the FtsZ ring (red) at the distal pole (Fig. 5N to P, arrow), where biogenesis of the second sporulation septum would likely have commenced. Thus, in the absence of σ^F-directed gene expression, SpoIIB-myc sequentially localized to each sporulation septum. Shortly before the completion of DNA translocation into each forespore, SpoIIB-myc was lost from the septum (Fig. 5Q to T, arrowheads). Thus, the assembly of SpoIIB in the septum and its subsequent loss are independent of both σ^F- and σ^E-directed gene expression and the onset of engulfment.

SpoIIB degradation is facilitated by its localization to division sites. To determine if the loss of localized SpoIIB-myc at the onset of engulfment correlated with its degradation or was solely due to exclusion from the septum, we performed a Western blot analysis to monitor SpoIIB-myc levels during sporulation (Fig. 7A). SpoIIB was first detected 1 h after the onset of sporulation, when levels of SpoIIB-myc were maximal. Ninety minutes after the onset of sporulation, a SpoIIB-myc breakdown product was seen (Fig. 7A, arrow 2) that was absent in strains lacking the SpoIIB-myc fusion, and levels of the protein gradually decreased until it was completely absent at $t_{3.0}$. Therefore, SpoIIB appears to be degraded early in engulfment, in correlation with its loss from polar septa. We next wanted to determine the stability of SpoIIB-myc under conditions in which it fails to localize, such as after depletion of FtsZ. In the absence of FtsZ, appearance of the putative SpoIIB-myc breakdown product was delayed by 2 h (until $t_{3.5}$) and SpoIIB-myc levels remained constant until at least $t_{3.5}$ (Fig. 7B). Thus, the instability of SpoIIB-myc depends on its localization to division sites.

DISCUSSION

***spoIIB* mutants display a transient engulfment defect.** We have used FM 4-64 staining and deconvolution microscopy to demonstrate that *spoIIB* mutants display a transient engulfment phenotype not previously described. This phenotype, consisting of a bulging of the forespore into the mother cell, is similar to that previously seen in *spoIID*, *spoIIM*, and *spoIIP* mutants, although *spoIIB* mutants are able to complete engulfment following bulge formation whereas *spoIID*, *spoIIM*, and *spoIIP* mutants are completely engulfment defective (Fig. 1). Electron microscopy showed that *spoIIB* mutants display an uneven dissolution of septal peptidoglycan and that engulfment occurs around residual peptidoglycan that often stretches most of the way across the mother cell. These results suggest that SpoIIB serves to regulate the dissolution of septal peptidoglycan, and they demonstrate that large amounts of residual septal peptidoglycan do not always inhibit membrane migration during engulfment, as has been observed in *spoIID*, *spoIIM*, and *spoIIP* mutants (13). Indeed a similar situation has been noted in wild-type *Bacillus sphaericus*, in which engulfment proceeds around residual septal peptidoglycan (15). Perhaps SpoIIB was a late addition to the engulfment machinery of *B. subtilis*, serving to increase the speed and efficiency of engulfment.

FIG. 5. Localization of SpoIIB-myc to the sporulation septum. Sporulation was induced by resuspension, and samples were prepared for immunofluorescence microscopy (see Materials and Methods). Chromosomes were visualized with DAPI (blue) (A, B, E, F, I to T, U, and V), and membranes were visualized by staining with FM 4-64 (red) (C, D, G, W, and X). The membranes appear less distinct in immunofluorescence experiments (which require chemical fixation and lysozyme treatment) than in living cells. However, the sporulation septum remains visible as a brightly staining region that is either flat (C [arrow] and G [arrow 1]), curved (G [arrow 2]), or, following the completion of engulfment, circular (G [arrow 3]). FITC-labeled secondary antibodies were used to visualize SpoIIB-myc (green) (B, D, F, H, J, L, N, P, R, T, V, and X), while Cy5-labeled secondary antibodies were used to visualize FtsZ (false-colored red) (K, L, O, P, S, and T). Overlays of SpoIIB-myc (green) and either DAPI (blue) (B, F, J, L, N, P, R, T, and V), FM 4-64 (red) (D, H, and X), FtsZ (red) (L, P, and T), or both DAPI (blue) and FtsZ (red) (L, M, and P) are shown. (A to D) Localization of SpoIIB-myc at $t_{1.5}$ in the wild type. The arrows point to localized SpoIIB-myc (B and D) in a sporangium with a partially translocated forespore chromosome (A) and a flat sporulation septum (C). The nonseptal, punctate staining is present in strains lacking the SpoIIB-myc fusion (not shown) and therefore represents nonspecific staining. The relatively high level of this staining is probably due to the low-level expression of the *spoIIB* gene (29), which decreases the specific signal. (E to H) Localization of SpoIIB-myc at $t_{2.5}$ in the wild type. Arrows 1 point to a sporangium that has not completely translocated its chromosome (E) and which still displays SpoIIB-myc localization (F and H). Arrows 2 point to a sporangium in which engulfment is almost complete (G), has completely translocated its chromosome (E), and may show only faint SpoIIB-myc localization (F and H). Arrows 3 indicate a sporangium that has completed engulfment (G) and lacks SpoIIB-myc (F and H). (I to L) Colocalization of SpoIIB-myc and FtsZ to partial sporulation septa in the wild type at $t_{1.5}$. The arrows point to one end of a sporangium that shows SpoIIB-myc (green) (J and L) colocalizing with a partially constricted FtsZ ring (red) (O and P). The arrowheads point to the FtsZ ring (K and L) at the second potential division site in the same sporangium; SpoIIB-myc is absent from this site. (M to P) Colocalization of SpoIIB-myc and FtsZ in sporangia lacking σ^F (Δ*spoIIAA-AC*) at $t_{1.5}$. The arrows and arrowheads indicate the two sites of polar septation in a single sporangium. The arrowheads point to a sporulation septum that is likely to be complete, since DNA translocation is well advanced (M) and FtsZ immunostaining is absent (O) but SpoIIB-myc localizes (M). The arrows indicate the second potential site of polar septation, which shows colocalization of SpoIIB-myc (N and P) and FtsZ (O and P) and little chromosome translocation (M). (Q to T) Colocalization of SpoIIB-myc and FtsZ in sporangia lacking σ^F (Δ*spoIIAA-AC*) at $t_{2.5}$. The arrows indicate a forespore with a partially translocated chromosome (Q) that has SpoIIB-myc localized throughout the septum (R and T). The arrowheads directly below the arrows indicate a forespore that has most of its chromosome translocated (Q) and lacks SpoIIB immunostaining (R and T). The arrowhead pairs point to a sporangium that has completely translocated both its chromosomes (Q) and no longer shows localization of SpoIIB-myc (R and T). These sporangia no longer display FtsZ localization (S and T). Panel Y shows a sketch of SpoIIB immunostaining (green) versus that of membranes (black) and chromosomes (blue). (U to X) SpoIIB-myc localization at $t_{1.5}$ after depletion of FtsZ from the P_{spac}*ftsZ* strain KP547. (W) FtsZ was depleted (see Materials and Methods), inhibiting cell division and causing the production of filaments. Only punctate SpoIIB-myc staining (V and X), similar to the background, is observed. (Y) Sketch of SpoIIB immunostaining in panels Q to T. SpoIIB immunostaining in the two sporangia indicated by arrows and arrowheads in panels Q to T is shown in green. Membranes are shown in black, while the chromosomes are shown in blue. The scale bar in panel X represents 2 μM.

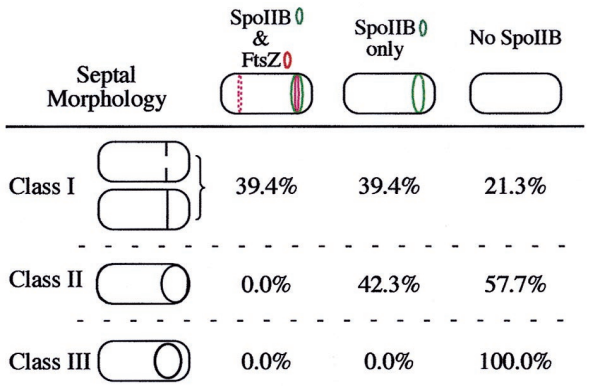

FIG. 6. Scoring of the localization patterns of SpoIIB-myc and FtsZ at different stages of engulfment and different times of the sporulation process. Samples were harvested 1.5 or 2.5 h after the onset of sporulation and processed for immunofluorescence microscopy. Sporangia were scored for localization of SpoIIB-myc and FtsZ and for the morphology of the polar septum, as revealed by FM 4-64 staining. Class I sporangia (flat polar septa) include both sporangia in which biogenesis of the sporulation septum is incomplete and those in which it is complete. The FtsZ ring distal to the active division site was sometimes lacking, for reasons that are unclear. Class II sporangia had curved sporulation septa, indicating that engulfment had commenced, while class III sporangia had completed engulfment. A total of 200 sporangia were scored from samples obtained from cultures at $t_{1.5}$ and $t_{2.5}$.

SpoIIB localizes to the sporulation septum during its biogenesis. To further investigate the role of SpoIIB, we determined its subcellular distribution during sporulation. We found that SpoIIB localizes to the sporulation septum during septal biogenesis, as evidenced by the colocalization of SpoIIB with the cell division protein FtsZ only at the growing septum and not at the inactive FtsZ ring present at the opposite pole of the same cell. It will be interesting to determine if SpoIIB recognizes some physical feature of the nascent sporulation septum or if it recognizes a cell division protein that is itself recruited to the division site either after or shortly before the onset of septal biogenesis.

Two sporulation-specific proteins, SpoIIE (2, 3, 16, 17, 22) and SpoIIGA (12), have previously been shown to localize to potential division sites, and several proteins have been shown to localize to the sporulation septum after its synthesis is completed (24, 33, 35, 36), but SpoIIB is the first shown to discriminate between the active site of septal biogenesis and the inactive division site in the same cell. Coincidentally, it has recently been observed that SpoIIIE, a protein required for the translocation of the chromosome into the forespore (49), shows a similar pattern of localization, initially colocalizing with FtsZ during septum biogenesis (M. D. Sharp, personal communication) and then localizing to the septal midpoint (41, 50). These observations raise the possibility that proteins required late in septation or after septation is complete can be localized to the septum after the onset of cell division. Since SpoIIB is incorporated into the forming septum, it is well positioned to facilitate the prompt and spatially regulated dissolution of septal peptidoglycan (as discussed further below).

SpoIIB is lost from the sporulation septum at the onset of engulfment. We noted that SpoIIB-myc localization was transient, since the protein no longer localized in sporangia that had commenced engulfment. The loss of SpoIIB from the septum did not require the dissolution of septal peptidoglycan, the onset of engulfment, or expression of any σ^F- or σ^E-dependent gene, because it occurred in mutants lacking σ^F. Thus, SpoIIB delocalization is not correlated with a particular morphological event but rather appears to occur at a set time after septal biogenesis is completed, even in the absence of further morphogenesis. SpoIIB was degraded during sporulation but could be stabilized if localization was inhibited (for example, by depletion of the cell division protein FtsZ). This suggests that either septation itself or localization to the septum is required for degradation of SpoIIB, similar to the situation observed for SpoIIE (22).

The role of SpoIIB in dissolution of septal peptidoglycan. In the absence of SpoIIB, septal thinning appears to occur throughout the septum and is often incomplete prior to the onset of engulfment. This suggests that SpoIIB contributes to the spatial regulation of septal peptidoglycan dissolution, ensuring that septal thinning commences in the middle of the septum and proceeds toward the edges. It also suggests a role for SpoIIB in the temporal regulation of septal peptidoglycan dissolution, ensuring that septal thinning is complete prior to the onset of engulfment. There are several possible mechanisms by which SpoIIB might contribute to the spatial and temporal regulation of septal thinning. First, SpoIIB might be an enzyme that degrades septal peptidoglycan, or it might regulate the activity of such an enzyme, ensuring that septal thinning commences in the middle of the septum and proceeds toward the edge. Alternatively, SpoIIB might recruit cell wall hydrolases to the polar septum. Because these hydrolases are likely to be produced under the control of σ^E (16), they would be synthesized after polar septation, while SpoIIB, which is localized to the polar septum while it is being synthesized, would be ideally positioned to recruit these proteins to the septum. Finally, it is also possible that SpoIIB is part of the cell division machinery and serves to modify the structure of the septal peptidoglycan to allow more efficient septal thinning. Further experiments are necessary to test these hypotheses.

Another look at the synergistic roles of SpoIIB and SpoVG in engulfment. In our study, we also investigated the interaction between SpoIIB and SpoVG (29). In agreement with previous studies, we found that a *spoVG* null mutant has a wild-type engulfment phenotype and that the *spoIIB spoVG*

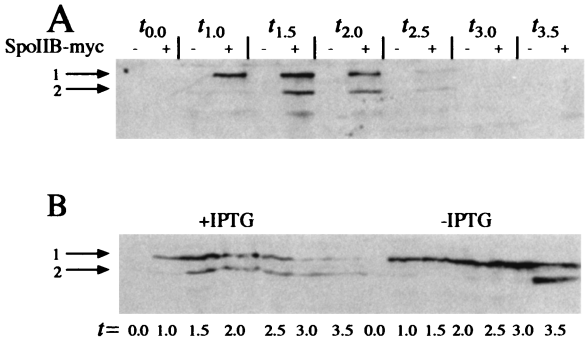

FIG. 7. Western blot analysis of SpoIIB-myc during engulfment. (A) Levels of SpoIIB-myc in the wild type. Samples from PY79, which lacks the *spoIIB-myc* fusion (indicated by minuses), and from KP545, which contains the *spoIIB-myc* fusion (indicated by pluses), were harvested and processed for Western blot analysis at the indicated times of the sporulation process. In KP545 (+), SpoIIB-myc is first detected at $t_{1.0}$ (arrow 1) but is rapidly degraded, showing a shorter-length product by $t_{1.5}$ (arrow 2) and completely disappearing by $t_{3.0}$. No signal is detected in the strain lacking the *spoIIB-myc* fusion (−). (B) Levels of SpoIIB-myc in the presence or absence of FtsZ. Strain KP547 carries *ftsZ* under the control of the IPTG-inducible P_{spac} promoter and the *spoIIB-myc* fusion. Cells which synthesize FtsZ are marked +IPTG, while those that have been depleted of FtsZ are marked −IPTG. When FtsZ is induced (+IPTG), SpoIIB is synthesized and degraded as in the wild type. However, in the absence of FtsZ (−IPTG), SpoIIB is stable until the last time point ($t_{3.5}$). Arrow 1 indicates full-length SpoIIB-myc, and arrow 2 indicates a shorter product that is likely to be a SpoIIB breakdown product.

double mutant has a more severe engulfment defect than the *spoIIB* single mutant. However, we also noted that *spoIIB spoVG* double-mutant cultures showed a variety of engulfment-related phenotypes, including sporangia in which the forespore had bulged into the mother cell or in which the engulfing membranes appeared to have initiated their migration around the forespore (Fig. 2M to P; Table 2). Recent studies by Sonenshein and colleague have suggested that SpoVG inhibits polar septation, since *spoVG* mutants initiate polar septation earlier than normal (30). We also found evidence to support the hypothesis that SpoVG inhibits division, since both the *spoVG* null mutant and the *spoIIB spoVG* double mutant produce sporangia with extra septa, either at the forespore distal pole (producing disporic sporangia) or at both midcell and polar sites (producing disporic sporangia with an extra septum at midcell [Fig. 2M and N]). Thus, SpoVG appears to inhibit cell division events subsequent to the formation of the sporulation septum, in addition to controlling the onset of polar septation.

Why do *spoVG* and *spoIIB* mutations act synergistically? First, it is possible that *spoVG* mutations cause alterations in sporangial physiology or structure that make engulfment more difficult in *spoIIB* mutants, perhaps as a direct consequence of the premature synthesis of the sporulation septum (30). The time prior to polar septation could be crucial for engulfment, either allowing structural alterations in the septal peptidoglycan or allowing synthesis of proteins whose functions are redundant to those of SpoIIB. Second, it is possible that the additional active and potential division sites in *spoVG* mutant sporangia cause the inappropriate localization of proteins essential for engulfment to these sites, rather than to the sporulation septum. In either case, because engulfment is already slow in *spoIIB* mutants, and because sporangia that fail to complete engulfment lyse (commencing around $t_{3.5}$ [our unpublished observations and references 31 and 43), the *spoVG* mutation need only slightly affect the speed or efficiency of engulfment in *spoIIB* mutants to dramatically decrease spore production.

A model for bulge formation. It has been proposed that a higher osmolarity in the forespore than in the mother cell may allow the forespore to grow larger during engulfment, possibly pushing the membranes around the forespore (10). Using time-lapse deconvolution microscopy (32), we found that, consistent with this model, the length of the forespore increased during engulfment by an average (± standard deviation) of 21.9% (± 11.9%) while the combined length of the two cells remained essentially constant, showing a slight decrease of 1.5% (± 3.1%) (see Materials and Methods and also the Pogliano lab website [http://www.biology.ucsd.edu/labs/pogliano]). While it is not yet clear that the growth of the forespore contributes to engulfment, it does provide a ready explanation for the formation of bulging forespores in mutants defective in the dissolution of septal peptidoglycan. In such mutants, forespore growth would exert pressure on a septum in which peptidoglycan hydrolysis was incomplete. For example, in *spoIID*, *spoIIM*, and *spoIIP* mutants, cell wall dissolution appears to occur only in the center of the septum (Fig. 1B). As the forespore grows, it will break through this weakened area to form a centrally localized and constricted bulge. In contrast, in *spoIIB* mutants, cell wall degradation appears to occur throughout the septum (Fig. 1C), and this will weaken the entire structure. Thus, as the forespore grows, the septum breaks and is breached by the forespore, resulting in both side and medial bulges. Significantly, while there is no engulfment in *spoIID*, *spoIIM*, and *spoIIP* mutants, *spoIIB* mutants are able to complete engulfment following bulge formation, despite the retention of peptidoglycan near the edges of the polar septum.

What implication do these findings have for the mechanism of engulfment? First, because the engulfing membranes can migrate around a large amount of residual peptidoglycan (Fig. 4B and C), peptidoglycan does not necessarily block migration of the engulfing membranes, as has been proposed to explain the engulfment defect of *spoIIP* mutants (13). Second, although membrane migration normally appears to commence at the edges of the septum following thinning of the septal peptidoglycan, migration must also be capable of starting in the middle of the septum, moving between the forespore membrane and the residual septal peptidoglycan in *spoIIB* mutant sporangia (Fig. 4Q). Finally, while some of our findings support the hypothesis that engulfment is facilitated by the growth of the forespore into the mother cell, the apparent uncoupling of these events in *spoIIB* mutants suggests the existence of additional mechanisms by which the membranes are driven around the forespore during engulfment.

ACKNOWLEDGMENTS

We are grateful to Petra Levin and Richard Losick for providing the FtsZ antibodies, to Nick Osborne for affinity purifying these antibodies, and to Terry G. Frey and Christian W. Renken for help in devising the alternative protocol for increasing membrane contrast during electron microscopy. We thank C. Lance Washington for technical assistance; Adam Driks for helpful advice; Kiyoteru Tokuyasu for discussions; Richard Losick, Katherine Lemon, Petra Levin, Alan Grossman, and Michael Carson for providing strains and plasmids; and Joe Pogliano for providing comments on the manuscript.

This work was supported by NIH grant GM-57045 to K.P., as well as by awards from the Arnold and Mabel Beckman Foundation and the Searle Scholars Program/The Chicago Community Trust. A.R.P. is supported by a MARC predoctoral fellowship from the NIH (GM19570-01).

REFERENCES

1. **Altschul, S. F., W. Gish, W. Miller, E. W. Myers, and D. J. Lipman.** 1990. Basic local alignment search tool. J. Mol. Biol. **215:**403–410.
2. **Arigoni, F., K. Pogliano, C. D. Webb, P. Stragier, and R. Losick.** 1995. Localization of a protein implicated in establishment of cell type to sites of asymmetric division. Science **270:**637–640.
3. **Barák, I., J. Behari, G. Olmedo, P. Guzmán, D. P. Brown, E. Castro, D. Walker, J. Westpheling, and P. Youngman.** 1996. Structure and function of the *Bacillus subtilis* SpoIIE protein and its localization to sites of sporulation septum assembly. Mol. Microbiol. **19:**1047–1060.
4. **Beall, B., and J. Lutkenhaus.** 1991. FtsZ in *Bacillus subtilis* is required for vegetative septation and for asymmetric septation during sporulation. Genes Dev. **5:**447–455.
5. **Bi, E. F., and J. Lutkenhaus.** 1991. FtsZ ring structure associated with division in *Escherichia coli*. Nature **354:**161–164.
6. **Bouché, J. P., and S. Pichoff.** 1998. On the birth and fate of bacterial division sites. Mol. Microbiol. **29:**19–26.
7. **Cutting, S., M. Anderson, E. Lysenko, A. Page, T. Tomoyasu, K. Tatematsu, T. Tatsuta, L. Kroos, and T. Ogura.** 1997. SpoVM, a small protein essential to development in *Bacillus subtilis*, interacts with the ATP-dependent protease FtsH. J. Bacteriol. **179:**5534–5542.
8. **Dubnau, D., and R. Davidoff-Abelson.** 1971. Fate of transforming DNA following uptake by competent *Bacillus subtilis*. J. Mol. Biol. **56:**209–221.
9. **Erickson, H. P.** 1997. FtsZ, a tubulin homologue in prokaryotic cell division. Trends Cell Biol. **7:**362–367.
10. **Errington, J.** 1993. *Bacillus subtilis* sporulation: regulation of gene expression and control of morphogenesis. Microbiol. Rev. **57:**1–33.
11. **Faguy, D. M., and W. F. Doolittle.** 1998. Cytoskeletal proteins: the evolution of cell division. Curr. Biol. **8:**R338–R341.
12. **Fawcett, P., A. Melnikov, and P. Youngman.** 1998. The *Bacillus* SpoIIGA protein is targeted to sites of spore septum formation in a SpoIIE-independent manner. Mol. Microbiol. **28:**931–943.
13. **Frandsen, N., and P. Stragier.** 1995. Identification and characterization of the *Bacillus subtilis spoIIP* locus. J. Bacteriol. **177:**716–722.
14. **Hayat, M. A.** 1986. Basic techniques for transmission electron microscopy, p. 182. Academic Press, Orlando, Fla.
15. **Holt, S. C., J. J. Gauthier, and D. J. Tipper.** 1975. Ultrastructural studies of sporulation in *Bacillus sphaericus*. J. Bacteriol. **122:**1322–1338.

16. **Illing, N., and J. Errington.** 1991. Genetic regulation of morphogenesis in *Bacillus subtilis*: roles of σ^E and σ^F in prespore engulfment. J. Bacteriol. **173:**3159–3169.
17. **King, N., O. Dreesen, P. Stragier, K. Pogliano, and R. Losick.** 1999. Septation, dephosphorylation, and the activation of sigma F during sporulation in *Bacillus subtilis*. Genes Dev. **13:**1156–1167.
18. **Kuroda, A., M. H. Rashid, and J. Sekiguchi.** 1992. Molecular cloning and sequencing of the upstream region of the major *Bacillus subtilis* autolysin gene: a modifier protein exhibiting sequence homology to the major autolysin and the *spoIID* product. J. Gen. Microbiol. **138:**1067–1076.
19. **Kuroda, A., Y. Sugimoto, T. Funahashi, and J. Sekiguchi.** 1992. Genetic structure, isolation, and characterization of a *Bacillus licheniformis* cell wall hydrolase. Mol. Gen. Genet. **234:**129–137.
20. **Lazarevic, V., P. Margot, B. Soldo, and D. Karamata.** 1992. Sequencing and analysis of the *Bacillus subtilis lytRABC* divergon: a regulatory unit encompassing the structural genes of the *N*-acetylmuramoyl-L-alanine amidase and its modifier. J. Gen. Microbiol. **138:**1949–1961.
21. **Levin, P., and R. Losick.** 1996. Transcription factor SpoOA switches the localization of the cell division protein FtsZ from a medial to a bipolar pattern in *Bacillus subtilis*. Genes Dev. **10:**478–488.
22. **Levin, P. A., R. Losick, P. Stragier, and F. Arigoni.** 1997. Localization of the sporulation protein SpoIIE in *Bacillus subtilis* is dependent upon the cell division protein FtsZ. Mol. Microbiol. **25:**839–846.
23. **Lewis, P. J., S. R. Partridge, and J. Errington.** 1994. σ factors, asymmetry, and the determination of cell fate in *Bacillus subtilis*. Proc. Natl. Acad. Sci. USA **91:**3849–3853.
24. **Londono-Vallejo, J.-A., C. Frehel, and P. Stragier.** 1997. *spoIIQ*, a forespore-expressed gene required for engulfment in *Bacillus subtilis*. Mol. Microbiol. **24:**29–39.
25. **Lopez-Diaz, I., S. Clarke, and J. Mandelstam.** 1986. *spoIID* operon of *Bacillus subtilis*: cloning and sequence. J. Gen. Microbiol. **132:**341–354.
26. **Lopilato, J., S. Bortner, and J. Beckwith.** 1986. Mutations in a new chromosomal gene of *Escherichia coli* K-12, *pcnB*, reduce plasmid copy number of pBR322 and its derivatives. Mol. Gen. Genet. **205:**285–290.
27. **Lutkenhaus, J.** 1993. FtsZ ring in bacterial cytokinesis. Mol. Microbiol. **9:**403–409.
28. **Lutkenhaus, J., and S. G. Addinall.** 1997. Bacterial cell division and the Z ring. Annu. Rev. Biochem. **66:**93–116.
29. **Margolis, P. S., A. Driks, and R. Losick.** 1993. Sporulation gene *spoIIB* from *Bacillus subtilis*. J. Bacteriol. **175:**528–540.
30. **Matsuno, K., and A. L. Sonenshein.** 1999. Role of SpoVG in asymmetric septation in *Bacillus subtilis*. J. Bacteriol. **181:**3392–3401.
31. **Piggot, P. J., and J. G. Coote.** 1976. Genetic aspects of bacterial endospore formation. Bacteriol. Rev. **40:**908–962.
32. **Pogliano, J., N. Osborne, M. D. Sharp, A. Abanes-De Mello, A. Perez, Y.-L. Sun, and K. Pogliano.** 1999. A vital stain for studying membrane dynamics in bacteria: a novel mechanism controlling septation during *Bacillus subtilis* sporulation. Mol. Microbiol. **31:**1149–1159.
33. **Pogliano, K., E. Harry, and R. Losick.** 1995. Visualization of the subcellular location of sporulation proteins in *Bacillus subtilis* using immunofluorescence microscopy. Mol. Microbiol. **18:**459–470.
34. **Pogliano, K., A. E. M. Hofmeister, and R. Losick.** 1997. Disappearance of the σ^E transcription factor from the forespore and the SpoIIE phosphatase from the mother cell contributes to establishment of cell-specific gene expression during sporulation in *Bacillus subtilis*. J. Bacteriol. **179:**3331–3341.
35. **Price, K. D., and R. Losick.** 1999. A four-dimensional view of assembly of a morphogenetic protein during sporulation in *Bacillus subtilis*. J. Bacteriol. **181:**781–790.
36. **Resnekov, O., S. Alper, and R. Losick.** 1996. Subcellular localization of proteins governing the proteolytic activation of a developmental transcription factor in *Bacillus subtilis*. Genes Cells **1:**529–542.
37. **Rong, S., M. S. Rosenkrantz, and A. L. Sonenshein.** 1986. Transcriptional control of the *Bacillus subtilis spoIID* gene. J. Bacteriol. **165:**771–779.
38. **Rosenbluh, A., C. D. B. Banner, R. Losick, and P. C. Fitz-James.** 1981. Identification of a new developmental locus in *Bacillus subtilis* by construction of a deletion mutation in a cloned gene under sporulation control. J. Bacteriol. **148:**341–351.
39. **Sandman, K., R. Losick, and P. Youngman.** 1987. Genetic analysis of *Bacillus subtilis spo* mutations generated by Tn*917*-mediated insertional mutagenesis. Genetics **117:**603–617.
40. **Setlow, B., N. Magill, P. Febbroriello, L. Nakhimovsky, D. E. Koppel, and P. Setlow.** 1991. Condensation of the forespore nucleoid early in sporulation of *Bacillus* species. J. Bacteriol. **173:**6270–6278.
41. **Sharp, M. D., and K. Pogliano.** 1999. An *in vivo* membrane fusion assay implicates SpoIIIE in the final stages of engulfment during *Bacillus subtilis* sporulation. Proc. Natl. Acad. Sci. USA **96:**14553–14558.
42. **Smith, K., and P. Youngman.** 1993. Evidence that the *spoIIM* gene of *Bacillus subtilis* is transcribed by RNA polymerase associated with σ^E. J. Bacteriol. **175:**3618–3627.
43. **Smith, K., M. E. Bayer, and P. Youngman.** 1993. Physical and functional characterization of the *Bacillus subtilis spoIIM* gene. J. Bacteriol. **175:**3607–3617.
44. **Steinmetz, M., and R. Richter.** 1994. Plasmids designed to alter the antibiotic resistance expressed by insertion mutations in *Bacillus subtilis*, through *in vivo* recombination. Gene **142:**79–83.
45. **Sterlini, J. M., and J. Mandelstam.** 1969. Commitment to sporulation in *Bacillus subtilis* and its relationship to development of actinomycin resistance. Biochem. J. **113:**29–37.
46. **Stragier, P., and R. Losick.** 1996. Molecular genetics of sporulation in *Bacillus subtilis*. Annu. Rev. Genet. **30:**297–341.
47. **Wang, X., J. Huang, A. Mukherjee, C. Cao, and J. Lutkenhaus.** 1997. Analysis of the interaction of FtsZ with itself, GTP, and FtsA. J. Bacteriol. **179:**5551–5559.
48. **Weiss, D. S., J. C. Chen, J.-M. Ghigo, D. Boyd, and J. Beckwith.** 1999. Localization of FtsI (PBP3) to the septal ring requires its membrane anchor, the Z ring, FtsA, FtsQ, and FtsL. J. Bacteriol. **181:**508–520.
49. **Wu, L. J., and J. Errington.** 1994. *Bacillus subtilis* SpoIIIE protein required for DNA segregation during asymmetric cell division. Science **264:**572–575.
50. **Wu, L. J., and J. Errington.** 1997. Septal localization of the SpoIIIE chromosome partitioning protein in *Bacillus subtilis*. EMBO J. **16:**2161–2169.
51. **Youngman, P., J. B. Perkins, and R. Losick.** 1984. A novel method for the rapid cloning in *Escherichia coli* of *Bacillus subtilis* chromosomal DNA adjacent to Tn*917* insertions. Mol. Gen. Genet. **195:**424–433.